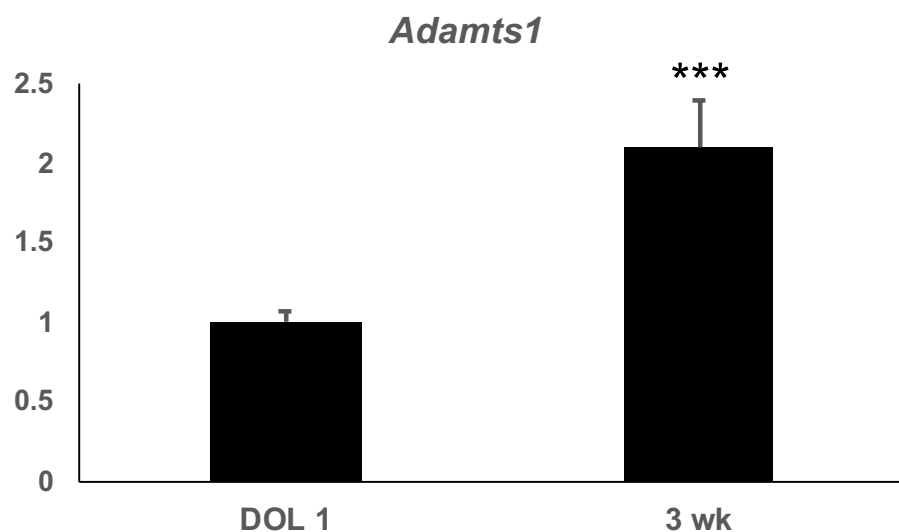
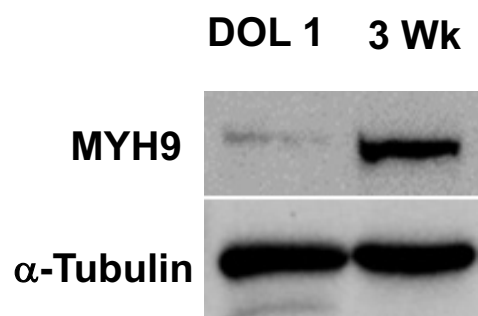


Supplemental Figure 1

A



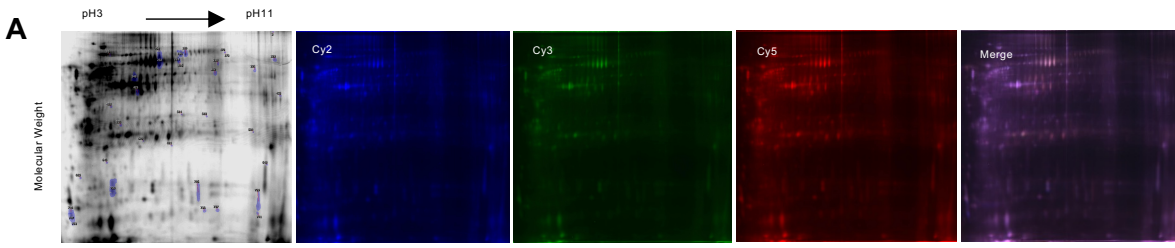
B



Supplemental Figure 1: Expression Levels of *Adamts1* and *Myh9* in Subcutaneous Adipose Depots

(A) RT-qPCR measuring the relative levels of *Adamts1* expression at DOL1 and 3 weeks of age. Adipose depots at DOL1 were too small to obtain sufficient protein to specifically detect ADAMTS1 by immunoblotting. (B) Immunoblots comparing MYH9 levels at DOL1 and 3 weeks of age. N=3. Error bars represent \pm SD from the mean. P values were calculated using t-tests *** P<0.001

Supplemental Figure 2



Top upregulated hits		Top downregulated hits	
Protein name	Gene	Protein name	Gene
cAMP-dependent protein kinase type I-alpha regulatory subunit	Prkar1a	TRIO and F-actin-binding protein	Triobp
Nuclear migration protein nudC	Nudc	WD repeat-containing protein 1	Wdr1
Protein disulfide-isomerase	P4hb	Cleavage stimulation factor subunit 2	Cstf2
Succinyl-CoA ligase [ADP-forming] subunit beta, mitochondrial	Sucl2	BAG family molecular chaperone regulator 3	Bag3
Thioredoxin domain-containing protein 5	Txndc5	Transgelin-2	Tagln2
Homer protein homolog 3	Homer3	Destrin	Dstn
Drebrin-like protein	Dbnl	Chloride intracellular channel protein 1	Clic1
Spectrin alpha chain, non-erythrocytic 1	Sptan1	Astrocytic phosphoprotein PEA-15	Pea15
Myosin-9	Myh9	COP9 signalosome complex subunit 4	Cops4
ATP synthase subunit beta, mitochondrial	Atp5b	NudC domain-containing protein 2	Nudcd2

KEGG Pathway analysis: Upregulated pathways					
Rank	Term	Count	p-value	Fold Enrichment	Benjamini
1	Citrate cycle (TCA cycle)	9	6.70E-06	8.4	8.00E-04
2	Glycolysis/Gluconeogenesis	12	1.60E-05	5.1	9.80E-04
3	Gap junction	13	3.10E-05	4.4	1.30E-03
4	Proteasome	8	9.90E-04	4.9	2.30E-02
5	Spliceosome	13	1.00E-03	3	2.10E-02

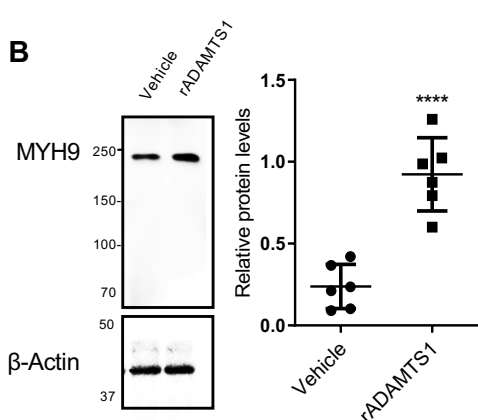
KEGG Pathway analysis: Downregulated pathways					
Rank	Term	Count	p-value	Fold Enrichment	Benjamini
1	Spliceosome	12	2.50E-05	4.9	2.10E-03
2	Glycolysis/Gluconeogenesis	9	4.60E-05	6.7	1.90E-03
3	Tight junction	12	5.60E-05	4.5	1.50E-03
4	Antigen processing and presentation	8	1.90E-03	4.5	3.00E-02
5	Regulation of actin cytoskeleton	12	3.20E-03	2.8	4.30E-02

Database of Annotation, Visualization, and Integrated Discovery (DAVID) Analysis v6.7

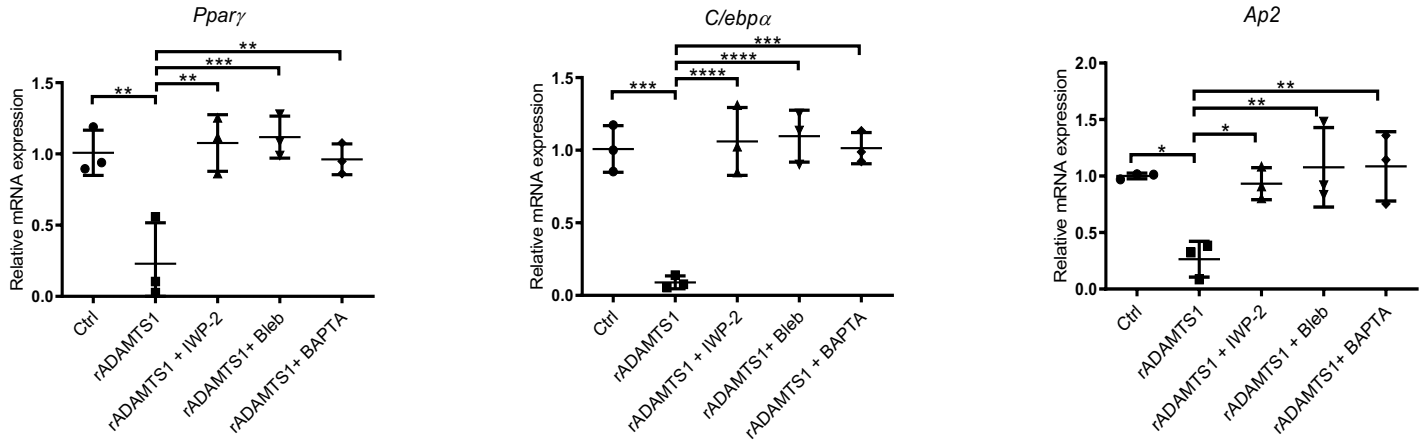
Rank	Category	Cluster Term	Count	Fold Change			
				Enrichment Score	p-value	Benjamini	FDR
1	GO:0008376	Cytoskeleton	106	27.02	2.10E-32	3.5	6.80E-30
		Cytoskeletal part	80		2.40E-26	3.9	4.00E-24
		Actin binding	38		7.40E-21	7.1	6.10E-19
		actin filament-based process	28		7.80E-14	6.1	3.20E-11
2	GO:0008377	actin cytoskeleton organization	27	14.05	1.20E-13	6.3	3.90E-11
		actin cytoskeleton	30		1.50E-13	5.5	5.90E-12
3	GO:0008378	Nucleotide-binding	141	11.62	6.90E-22	2.2	3.10E-19
		Purine nucleotidetriphosphate binding	107		2.00E-13	2	1.50E-11
		ATP binding	83		1.50E-09	2	5.60E-08
4	GO:0008379	Intermediate filament	22	10.91	8.00E-11	6	2.60E-09
		Intermediate filament cytoskeleton	22		1.20E-10	5.9	3.60E-09
5	GO:0008380	Contractile Fiber	22	9.87	4.70E-14	8.7	3.00E-12
		Myofibril	20		2.30E-12	8.2	8.30E-11
6	GO:0008381	Cellular macromolar complex subunit organization	35	8.61	8.80E-16	5.5	1.40E-12
		GTPase Activity	23		1.60E-11	6.2	1.00E-09
		Microtubule-based movement	17		6.30E-09	6.5	7.40E-07
7	GO:0008382	protein complex biogenesis/assembly	21	8.61	1.90E-06	3.6	1.10E-04
		Gap Junction	13		1.70E-04	3.7	3.60E-03
8	GO:0008383	Vesicle	33	7.65	8.55E-06	2.4	9.60E-05
		cytoplasmic membrane-bounded vesicle	28		1.70E-04	2.5	1.00E-04
		mRNA processing	27		4.50E-09	4	5.60E-07
9	GO:0008384	RNA binding	47	7.37	5.50E-08	2.4	1.80E-06
		mRNA metabolic process	27		8.40E-08	3.4	7.60E-06
10	GO:0008385	RNA splicing	20	6.16	1.20E-06	3.8	7.70E-05
		Cell cortex	20		8.70E-10	5.9	2.20E-08
11	GO:0008386	glucose metabolic process	20	6.16	3.50E-09	5.5	5.10E-07
		generation of precursor metabolites and energy	27		4.10E-09	4	5.60E-07
		glycolysis	11		1.40E-07	9.6	1.10E-05
12	GO:0008387	Glycolysis/Gluconeogenesis	13	6.16	1.60E-05	4.6	6.60E-04
		Pyruvate metabolism	7		6.00E-03	4.2	5.60E-02

Supplemental Figure 2: Proteomic Analysis of the Response to rADAMTS1

(A) Whole cell proteome analysis of preadipocytes treated with recombinant ADAMTS1 compared to vehicle treatment control using two-dimensional fluorescence difference gel electrophoresis (2D-DIGE). **(B)** Immunoblot (left) and quantification (right) of the induction of MYH9 in response to rADAMTS1 ($n=6$). Error bars represent \pm SD from the mean. P values were calculated using t-tests **** P<0.0001



Supplemental Figure 3

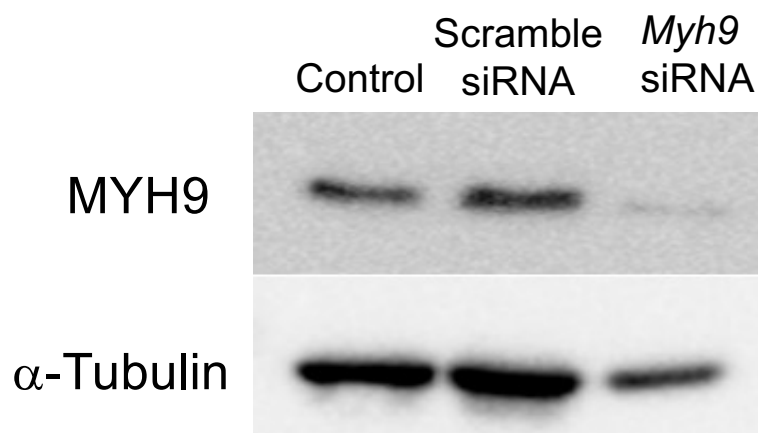


Supplemental Figure 3: Adamts1-Wnt-Myh9 Pathway Regulates Adipogenesis

RT-qPCR quantifying the expression levels of markers of adipogenesis in APCs treated with rADAMTS1 alone and with IWP-2, Bleb or BAPTA (n=3).

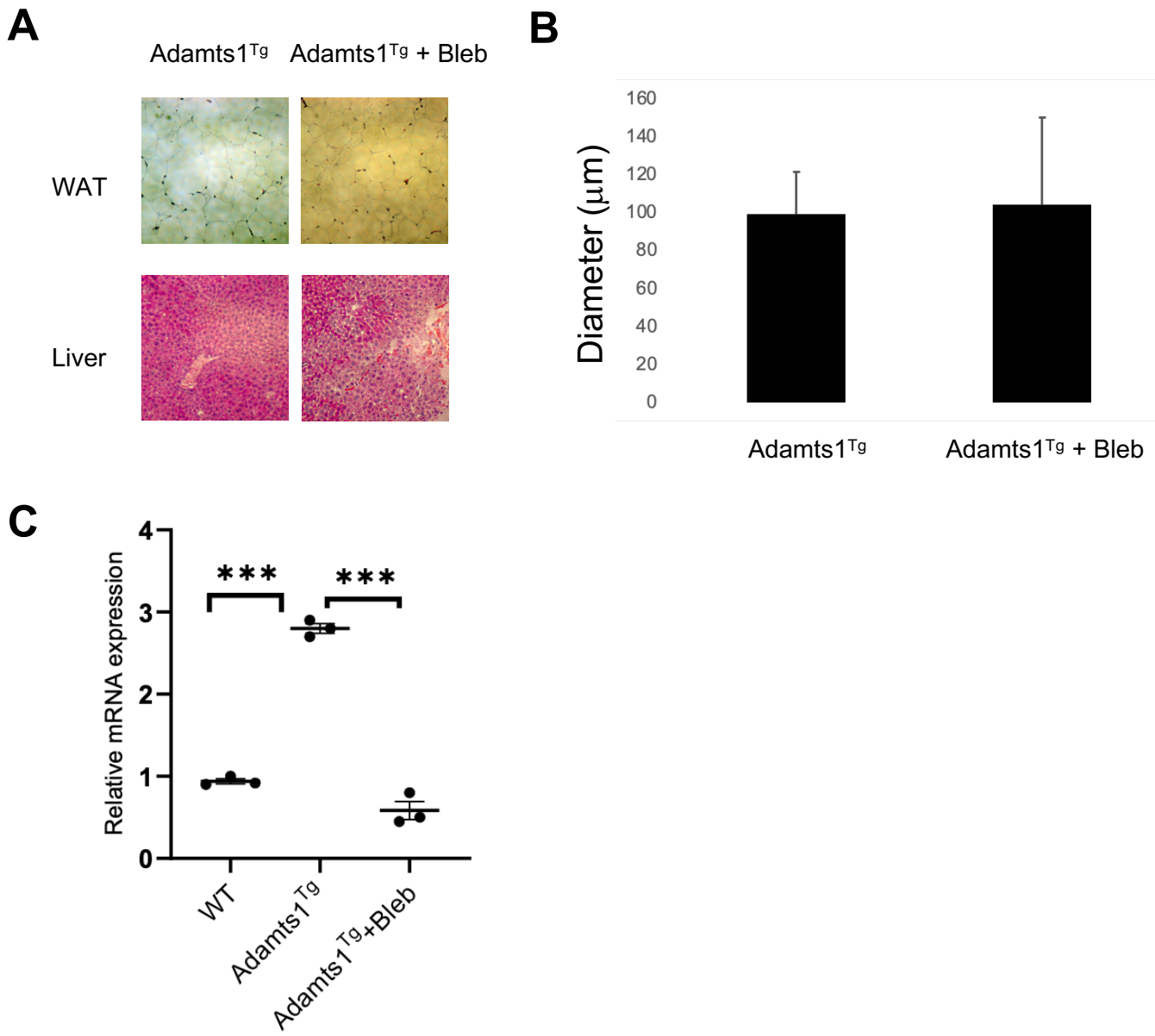
Error bars represent \pm SD from the mean. P values were calculated using t-tests followed by Bonferroni corrections. *p<0.05, **p<0.01, ***p<0.001, ****p<0.0001.

Supplemental Figure 4



Supplemental Figure 4: Validation of Myh9 knockdown using siRNA:
Immunoblots from preadipocyte cell lysates harvested 48 hrs after being transfected with either scramble or *Myh9* specific siRNA, demonstrating that *Myh9* specific siRNA results in ~60% knockdown in MYH9 levels.

Supplemental Figure 5



Supplemental Figure 5: Bleb treatment of Adamts1^{Tg} mice:

(A) Images of histological sections from WAT and liver. (B) Quantification of adipocyte size (μm) using ImageJ analysis of the histological sections. There is no statistical difference in the adipocyte size. (C) RT-qPCR quantifying the expression level of *Myh9* in WAT ($n=3$)

Error bars represent $\pm\text{SD}$ from the mean. P values were calculated using t-tests followed by Bonferroni correction. *** $P<0.001$